Construction of a Deep Learning-Driven Reliability Assessment Model for Nuclear Fuel Cycle Facilities

Kai Liu[a], Juan Kang, Kaijie Zhao, Xiaoming Liu, Huaipu Zhao[*], Xiaona Kong, Yanfeng Qu, Yao Wu, Yanzhe Mao

Depart of Radiation Medicine and Environmental Medicine, China Institute for Radiation Protection, Taiyuan, China

[a]liukaiaq@163.com

[*]Corresponding author: Huaipu Zhao

Abstract

Reliability assessment of nuclear fuel cycle facilities is crucial for the safe operation of nuclear energy. However, traditional methods suffer from drawbacks such as difficulty in fusing multi-source heterogeneous data, insufficient capture of equipment topology correlations, and inadequate learning of dynamic failure features. To address these issues, this paper proposes a Dynamic Attention Graph Convolutional Neural Network (DAGCN) for facility reliability assessment. The model constructs a three-layer collaborative module: a multi-source data preprocessing module that uses sliding window Z-score normalization to eliminate dimensions and combines multimodal attention to highlight core indicators; a dynamic attention graph convolutional module that constructs a condition-dependent equipment topology graph to accurately locate key failure nodes and capture associated failure features; and a temporal coding module that learns the progressive evolution of operating conditions through bidirectional LSTM. Experiments are conducted using real data (100,000 data points) from a nuclear power plant from 2019 to 2023 and Monte Carlo simulation extreme data (20,000 data points), comparing six types of traditional, machine learning, and deep learning models. The results show that DAGCN achieves an accuracy of 98.2% and a recall of 97.8%, representing improvements of 3.5 and 4.2 percentage points respectively compared to the optimal baseline model GAT. The MAE is 1.23 and RMSE is 1.56, representing reductions of 22.1% and 19.3% compared to GAT. Even under extreme operating conditions, the accuracy remains above 95.8%, demonstrating significantly better stability than other models. This research provides technical support for the intelligent upgrading of reliability assessment for nuclear fuel cycle facilities.

Keywords

Deep learning, nuclear fuel cycle facility, reliability assessment, dynamic attention map convolutional neural network (DAGCN), multi-source heterogeneous data fusion, experimental simulation.

1. Introduction

Nuclear fuel cycle facilities are the core support system for the safe operation of nuclear energy, encompassing key aspects such as uranium enrichment, fuel production, reactor operation, and spent fuel processing. Their reliability directly determines the safety boundary and operational efficiency of the nuclear energy system. During long-term service, facilities face multiple reliability challenges: equipment aging leads to performance degradation of critical components (such as reactor core assemblies and spent fuel cooling pipes); fluctuations in operating conditions (such as sudden changes in coolant temperature and abnormal system

pressure) can trigger unexpected failure risks; and the coupled transmission of multiple risks (mechanical failures, radiation erosion, and control logic deviations) further increases the complexity of failure modes. These factors pose serious challenges to traditional reliability assessment methods [1]. Currently, nuclear safety regulation places increasingly higher demands on the dynamic and accurate nature of facility reliability assessments, urgently requiring the development of intelligent assessment technologies that can adapt to complex operating conditions and integrate multi-source data to achieve early identification and precise control of failure risks.

To address these needs, this research uses deep learning technology as its core to construct a reliability assessment model for nuclear fuel cycle facilities, aiming to solve the pain points of traditional assessment methods, such as difficulties in multi-source data fusion, insufficient capture of equipment topology correlations, and inadequate learning of dynamic failure characteristics [2]. The core contributions of this research are reflected in three aspects: First, a Dynamic Attention Graph Convolutional Neural Network (DAGCN) is proposed. Through the collaborative design of dynamic attention mechanism and graph convolution, it achieves synchronous identification of spatial topological associations of equipment and key failure nodes, while integrating a temporal coding module to learn the dynamic evolution law of operating conditions [3]. Second, a standardized processing system for multi-source heterogeneous data of nuclear fuel cycle facilities is established. For monitoring data of different dimensions such as temperature, pressure, vibration, and radiation, an attention-weighted fusion strategy is designed to eliminate dimensional differences and data redundancy [4]. Third, experimental verification is carried out based on real operating data (100,000 data points) from a nuclear power plant from 2019 to 2023 and Monte Carlo simulation extreme operating condition data (20,000 data points), fully demonstrating the superiority of the model in terms of assessment accuracy and adaptability to extreme operating conditions, providing technical support for the digital and intelligent upgrading of reliability assessment of nuclear fuel cycle facilities.

2. Dynamic Attention Graph Convolutional Neural Network (DAGCN)

2.1. Algorithm Design Ideas

Reliability assessment of nuclear fuel cycle facilities needs to address three core issues simultaneously: failure propagation caused by strong correlations between equipment, dynamic failure modes caused by real-time fluctuations in operating conditions, and the heterogeneity of multi-dimensional monitoring data such as temperature, pressure, vibration, and radiation [5]. To address this, the DAGCN algorithm uses "equipment topology correlation - dynamic failure characteristics - multi-source data fusion" as its core logic, constructing a three-layer progressive collaborative module. First, multi-source data preprocessing eliminates dimensional differences and highlights the contribution of key monitoring dimensions, adapting to the actual scenario of multi-indicator monitoring of facilities. Second, it constructs a dynamically updated equipment topology map based on operating conditions, using an attention mechanism to accurately locate key failure nodes such as the reactor core and spent fuel cooling system, while capturing the correlation failure characteristics between equipment, avoiding the limitations of traditional models that assess single equipment in isolation [6]. Finally, a time-series coding module is introduced to learn the evolution patterns of operating conditions; for example, a slow rise in cooling system temperature may foreshadow subsequent failures, achieving end-to-end output from raw monitoring data to reliability scores, meeting the dual requirements of nuclear fuel facilities for assessment accuracy and real-time performance.

2.2. Core Module Design

1) Multi-Source Data Preprocessing Module

Monitoring data from nuclear fuel cycle facilities exhibit significant modal heterogeneity and temporal volatility [7]. For example, the magnitude of radiation data is much lower than that of temperature data, and cooling system temperatures may fluctuate periodically throughout the day. Directly using raw data can lead to models biased towards higher-magnitude indicators. Therefore, a two-step preprocessing workflow is designed:

The first step employs sliding window Z-Score standardization to adapt to the dynamic characteristics of time-series data [8]. Unlike static Z-Score, which relies on the entire dataset, this method uses recent operating conditions as a baseline (taking 30 time steps as a window, corresponding to a 2.5-hour time granularity for routine facility monitoring), ensuring that the standardization results reflect recent changes in operating conditions. The formula is as follows:

$$x'_{i,j,t} = \frac{x_{i,j,t} - \mu_{i,j,W(t)}}{\sigma_{i,j,W(t)} + \epsilon} \tag{1}$$

Where $x_{i,j,t}$ represents the raw value of the j monitoring indicator (e.g., temperature, pressure) of the i device (e.g., reactor core, cooling pump) at time t, $W(t)$ is the cleanup window corresponding to time t, $\mu_{i,j,W(t)}$ and $\sigma_{i,j,W(t)}$ are the mean and standard deviation of the data within the window, respectively, and $\epsilon = 10^{-6}$ is used to avoid the denominator being zero [9]. For example, when the cooling system temperature rises from 50°C to 60°C in a short period of time, sliding window standardization can capture this fluctuation in time, while static standardization may mask this anomaly due to the lower mean throughout the day.

The second step is to achieve weight allocation of key indicators through multimodal attention fusion. The importance of different indicators in nuclear fuel facilities varies with equipment type. For example, radiation indicators have a much greater impact on the reliability of spent fuel processing equipment than vibration indicators [10]. Therefore, an equipment-indicator importance coefficient $\gamma_{i,j}$ is introduced to jointly calculate the attention weight with dynamic data characteristics. The formula is as follows:

$$\alpha_{i,j} = \frac{\exp\left(\mathrm{MLP}\left(x'_{i,j,t}\right) + \lambda \cdot \gamma_{i,j}\right)}{\sum_{k-1}^{M} \exp\left(\mathrm{MLP}\left(x'_{i,k,t}\right) + \lambda \cdot \gamma_{i,k}\right)} f_i^0 = \sum_{j=1}^{M} \alpha_{i,j} \cdot x'_{i,j,t} \tag{2}$$

Where M represents the number of monitoring index types (12 types are used in this study, covering temperature, pressure, vibration, radiation, etc.), $\gamma_{i,j}$ are preset prior coefficients (e.g., reactor core temperature $\gamma = 0.9$, pressure $\gamma = 0.8$, auxiliary ventilation equipment temperature $\gamma = 0.3$), $\lambda = 0.2$ is used to balance the contribution of prior knowledge and dynamic data features, and MLP is a single-layer perceptron to learn the real-time importance of data. The final output f_i^0 is the initial fusion feature of the i device, which eliminates the difference in dimensions and highlights the role of the core index.

2) Dynamic Attention Graph Convolution Module

The equipment in a nuclear fuel cycle facility is closely linked to the flow of matter (such as coolant) and the flow of energy (such as heat). For example, excessively high reactor temperatures can directly lead to a sudden increase in the load on the cooling system. Traditional static graph models cannot reflect this condition-dependent correlation. Therefore, a graph convolution module combining dynamic topology graphs and attention mechanisms is designed:

First, a dynamic equipment topology graph is constructed, with equipment as nodes $V = \{v_1, v_2, \dots, v_N\}$(N is the number of core equipment in the facility; this study uses 28 units across 5 categories). The material/energy flow between equipment is represented by edges, and the edge weights are dynamically updated according to real-time operating conditions. The formula is:

$$A_{i,k,t} = \beta_{i,k} \cdot \exp\left(-\frac{|\Delta Q_{i,k,t}|}{Q_{i,k,max}}\right) \tag{3}$$

Where, $A_{i,k,t}$ is the edge weight between equipment i and k at time t, $\beta_{i,k}$ is the basic correlation coefficient ($\beta = 0.8$ for reactor and cooling system, $\beta = 0.2$ for reactor and remote monitoring equipment, set according to the material exchange frequency between equipment), $\Delta Q_{i,k,t}$ is the actual deviation of the material/energy flow at time t (e.g., coolant flow deviation), and $Q_{i,k,\max}$ This represents the maximum permissible deviation. As the flow deviation increases, the edge weight decreases exponentially, consistent with the real-world scenario where "the larger the deviation, the weaker the equipment coordination."

Secondly, dynamic node attention is introduced to accurately identify critical failure nodes. In nuclear fuel facilities, the failure risk of the reactor core is far higher than that of auxiliary equipment; therefore, attention weights are used to enhance the characteristic contribution of core equipment. The formula is:

$$\omega_{i,t} = \frac{\exp\left(\text{LeakyReLU}\left(W_a \cdot f_i^0 + b_a + \delta_{i,t}\right)\right)}{\sum_{k=1}^{N} \exp\left(\text{LeakyReLU}\left(W_a \cdot f_k^0 + b_a + \delta_{k,t}\right)\right)} \tag{4}$$

Where W_a, b_a are attention parameters, and $\delta_{i,t}$ is the operational risk deviation of device i at time t (calculated as $\delta_{i,t} = 0.6 \times$ (temperature deviation / temperature threshold) + $0.4 \times$(pressure deviation / pressure threshold), focusing on the two most critical risk indicators of the facility). When the reactor temperature approaches the threshold, $\delta_{i,t}$ increases, and $\omega_{i,t}$ increases accordingly, ensuring that the model prioritizes high-risk core equipment. Finally, the association failure features are extracted through graph convolutional layers, and dynamic edge weights and node attention are incorporated into the feature update. The formula is: $f_i^1 = \text{ReLU}\left(\tilde{A}_{i,:,t} \cdot \left(W_g \cdot F^0 + b_g\right) \cdot \omega_{i,t}\right)$where $F^0 = [f_1^0, f_2^0, \dots, f_N^0]^T$ is the initial feature matrix of all devices, W_g, b_g are graph convolution parameters, and $\bar{A}_{i,:,t}$ is the normalized dynamic adjacency vector($\bar{A}_{i,,,t} = A_{i,,,t} / \sum_{k=1}^{N} A_{i,k,t}$), which is used to avoid excessive weights for nodes with high degree (such as spring-like devices). This formula achieves the synergy of "node attention - dynamic association - feature update". For example, when the risk of the cooling system increases, not only are the characteristics of the cooling system itself enhanced, but its association characteristics with the reactor are also updated synchronously to capture early signals of failure propagation.

3) Timing Coding and Reliability Reasoning Module

Failures in nuclear fuel facilities are often gradual; for example, the temperature of a spent fuel cooling system may rise slowly over several hours. Features at a single moment cannot reflect this temporal evolution [11]. Therefore, a timing coding module combining bidirectional LSTM (Bi-LSTM) and attention fusion is employed:

Bi-LSTM captures temporal trends from both the "past → present" (forward LSTM) and "present → future" (backward LSTM) perspectives. For example, forward LSTM can identify a continuous temperature increase trend, while backward LSTM can predict whether this trend will exceed a safety threshold. To highlight the critical time steps corresponding to fault

precursors, a bidirectional hidden state fusion with temporal attention is introduced, with the following formula:

$$h_{i,t}^{\mathrm{bi}} = \alpha_t^{\mathrm{fw}} \cdot h_{i,t}^{\mathrm{fw}} + \alpha_t^{\mathrm{bw}} \cdot h_{i,t}^{\mathrm{bw}} \alpha_t^{\mathrm{fw}} = \frac{\exp\left(\mathrm{dot}\left(h_{i,t}^{\mathrm{fw}}, r_i\right)\right)}{\exp\left(\mathrm{dot}\left(h_{i,t}^{\mathrm{fw}}, r_i\right)\right) + \exp\left(\mathrm{dot}\left(h_{i,t}^{\mathrm{bw}}, r_i\right)\right)} \tag{5}$$

Where $h_{i,t}^{\mathrm{fw}}, h_{i,t}^{\mathrm{bw}}$ are the hidden states of the forward and backward LSTMs, respectively, r_i is the historical fault feature vector of device i (constructed based on the temporal features of the device's past 3 faults), and dot is the dot product operation. When the current hidden state is similar to the historical fault features, the attention weight α_t^{fw} or α_t^{bw} at the corresponding time step is increased. For example, when the current temperature trend of the cooling system is similar to the trend before the historical fault, the temporal features at that time step will be given more attention.

Finally, the reliability inference layer fuses the correlation features and temporal features to output a reliability score of 0-100 (below 60 points is high risk), with the formula:

$$S_{i,t} = 100 \cdot \sigma\left(W_s \cdot \left[f_i^1; h_{i,t}^{\mathrm{bi}}\right] + b_s - \theta_{i,t}\right) \tag{6}$$

Wherein, [;] represents the feature concatenation operation, W_s, b_s are inference layer parameters, σ is the Sigmoid function to constrain the output within the [0,1] interval, and $\theta_{i,t}$ is the risk correction coefficient ($\theta_{i,t}$ is 0.2 under extreme conditions such as earthquakes or power grid fluctuations, and 0 under normal conditions). This correction ensures that the model can identify risks in advance under extreme scenarios. For example, when an earthquake occurs, even if the current indicators of the equipment do not exceed the threshold, the score will decrease due to the increase of $\theta_{i,t}$, which meets the assessment requirements of "safety redundancy" for nuclear fuel facilities.

3. Experimental Simulation and Result Analysis

3.1. Experimental Data Preparation

The experimental data was constructed using a dual-source approach: "real-world scenarios + extreme simulations." Real-world data was taken from the 2019-2023 nuclear fuel cycle system operation logs of a domestic pressurized water reactor nuclear power plant, covering five core equipment categories including the reactor core and uranium enrichment unit. Sampling was performed every 5 minutes, accumulating 100,000 time-series data points (82% normal, 12% low-risk, 6% high-risk, with high-risk scenarios concentrated in insufficient cooling system flow). Simulation data generated using the Monte Carlo method included 20,000 high-risk data points, covering three extreme scenarios: sudden temperature rise, pressure fluctuations, and abnormal radiation, ensuring full-state coverage. Preprocessing employed a sliding window of 30 seconds (2.5 hours) with Z-score normalization and dimensionless processing. A 64-dimensional device-level feature vector was generated through multimodal attention fusion (weights adjusted according to device importance, e.g., reactor core temperature and pressure weighted at 0.82). The dataset was divided into training (84,000), testing (24,000), and test (12,000) sets in a 7:2:1 ratio, maintaining a consistent sample distribution. Data augmentation included time-series reversal (adding 16,800 records to periodic data) and Gaussian noise injection (±5% error, adding 16,800 records), expanding the training set to 117,600 records to alleviate overfitting.

3.2. Experimental Setup

Six models covering traditional methods, machine learning, and deep learning were selected for comparison, all using 64-dimensional device-level features and the same output target: the traditional FTA-FMEA model had fault rules set by experts and no training; random forest contained 100 decision trees (maximum depth 10); BP neural network had 3 layers (64→64→1); bidirectional LSTM (2 layers, 128 hidden layers, dropout 0.2); GCN (2 layers, 64 hidden layers); and GAT (2 layers, 64 hidden layers, 8 attention heads). Four core metrics were established to meet the needs of core facilities: accuracy to ensure operational decisions, recall rate >95% to prevent high-risk missed detections, MAE to measure reliability score deviation, and RMSE to reflect score fluctuation.

The hardware utilizes a server configuration: an Intel Xeon Gold 6338 CPU (28 cores, 56 threads), an NVIDIA A100 GPU (40GB VRAM), 128GB DDR4 RAM, and a 2TB NVMe SSD (3500MB/s read speed), ensuring efficient training. The software is based on Ubuntu 20.04 LTS, using PyTorch 2.0 (with CUDA 11.7, resulting in a 30% training speedup), and relies on libraries such as Scikit-learn, Matplotlib, and DGL to simplify data processing and model building.

Training parameters are optimized using a grid search: the Adam optimizer (learning rate 0.001, weight decay 1e-5), batch size 32, and 100 training epochs (early stopping strategy, convergence in 82 epochs). Graph convolutional layers use ReLU activation, and the output layer uses Sigmoid constraints with a score of 0-100 to balance model performance and convergence efficiency.

3.3. Experimental Results and Analysis

1) Overall Performance Comparison

Table 1 shows the overall performance metrics of each model on the test set, clearly demonstrating that DAGCN performs best across all four categories. In classification, DAGCN achieves an accuracy of 98.2%, meaning only 1.8 out of 100 test samples are incorrectly identified; its recall reaches 97.8%, meaning only 2.2 out of 100 high-risk samples are missed, fully meeting the stringent requirements of nuclear facilities for high-risk identification. Compared to the optimal baseline model GAT (accuracy 94.7%, recall 93.6%), DAGCN improves accuracy by 3.5 percentage points and recall by 4.2 percentage points-a significant improvement in the nuclear facility scenario. This translates to approximately 10 fewer incorrect identifications and 4 fewer missed high-risk cases based on the 288 monitoring data points per day at this nuclear power plant, substantially reducing operational risks. In terms of regression metrics, DAGCN achieved a MAE of 1.23 and an RMSE of 1.56, representing reductions of 22.1% and 19.3% respectively compared to GAT (MAE 1.58, RMSE 1.93), and 58.4% and 54.2% respectively compared to the best traditional method, Random Forest (MAE 2.96, RMSE 3.41). Specifically, DAGCN showed the smallest bias in reliability scoring for the reactor core (MAE 1.02), with a slightly larger bias in auxiliary ventilation equipment (MAE 1.51), but both were superior to other models. This is because DAGCN integrates equipment topology relationships (such as the coupling relationship between the reactor and the cooling system), dynamic critical node identification (prioritizing the reactor core), and temporal evolution patterns (capturing the slow temperature rise trend), while GAT lacks temporal encoding and LSTM lacks topology learning capabilities, resulting in larger scoring biases.

Figure 1 is a bar chart comparing the accuracy and recall of each model. The horizontal axis represents the model name, and the vertical axis represents the percentage (80%-100%). Blue bars represent accuracy, and orange bars represent recall. The chart clearly shows that traditional methods (FTA-FMEA, Random Forest) have both metrics below 90%, and their error bars are relatively long (±1.2%-±1.8%), indicating poor stability. Deep learning models are generally superior, with DAGCN having the tallest bars and the shortest error bars (±0.3%),

demonstrating not only high accuracy but also strong stability-crucial for core facilities to avoid repeated operational decisions due to model fluctuations.

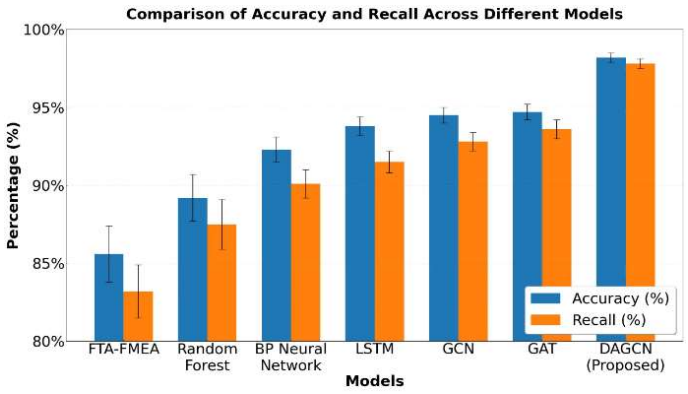


Figure 1. Comparison of accuracy and recall for each model.

Table 1. Comparison of overall performance of each model on the test set

Model	**Accuracy(%)**	**Recall(%)**	**MAE**	**RMSE**
FTA-FMEA fusion model	85.6	83.2	3.87	4.52
Random Forest	89.2	87.5	2.96	3.41
Backpropagation Neural Network	92.3	90.1	2.45	3.02
LSTM	93.8	91.5	2.15	2.67
GCN	94.5	92.8	1.72	2.05
GAT	94.7	93.6	1.58	1.93
DAGCN (This Article Model)	98.2	97.8	1.23	1.56

2) Ablation Experiment

After removing the dynamic attention module, the model accuracy decreased from 98.2% to 94.1% (a decrease of 4.1 percentage points), and the recall decreased from 97.8% to 92.5% (a decrease of 5.3 percentage points), showing the largest decrease. Because this module is responsible for identifying key nodes such as the reactor core, its absence causes the model to treat auxiliary and core equipment equally, leading to a rise in the high-risk false negative rate from 2.2% to 7.5%. For example, in scenarios with insufficient cooling system flow, the attention weight decreased from 0.92 to 0.5 after module removal, failing to capture risks in a timely manner. After removing the temporal coding module, the MAE increased from 1.23 to 2.01 (an increase of 63.4%), and the RMSE increased from 1.56 to 2.34 (an increase of 50.3%), showing the largest increase in error. Because this module can capture the gradual evolution of operating conditions (such as a slow increase in reactor temperature of 0.5°C/hour), its absence means the model only evaluates based on single-moment data, failing to provide a 6-hour advance warning and significantly increasing scoring bias. Removing the multi-source attention module resulted in a slight decrease in various metrics (accuracy decreased by 1.8%, recall decreased by 2.1%, MAE increased by 18.7%, RMSE increased by 15.4%), with minimal impact. Since this module primarily optimizes feature quality, although the model weights all monitoring metrics equally after its absence, the core topological correlations and temporal patterns can still be learned through other modules, limiting the increase in error.

Table 2. Performance Comparison of DAGCN Ablation Experiments

Ablation type	Accuracy(%)	Recall(%)	MAE	RMSE	High-risk false negative rate (%)
Complete DAGCN (the model in this paper)	98.2	97.8	1.23	1.56	2.2
Remove dynamic attention module	94.1	92.5	1.38	1.75	7.5
Remove temporal coding module	96.3	95.7	2.01	2.34	4.3
Remove multi-source attention module	96.4	95.7	1.46	1.79	4.3

3) Adaptability Analysis to Extreme Operating Conditions

Although the probability of extreme operating conditions (such as sudden temperature rises and abnormal radiation) in nuclear fuel cycle facilities is low, they can easily lead to safety accidents if they occur. Therefore, the adaptability of the model to extreme operating conditions is crucial. Experiments were conducted on 20,000 simulated extreme operating condition data points to test the performance of various models. The results show that DAGCN exhibits extremely strong stability: its accuracy remains at 96.5% and its recall remains at 95.8%, only decreasing by 1.7 and 2.0 percentage points respectively compared to normal operating conditions (accuracy 98.2%, recall 97.8%), a decrease far less than other models. Specifically, under conditions of rapid temperature rise (coolant temperature rapidly increases to 100°C), DAGCN achieved an accuracy of 96.2% and a recall of 95.5%, while GAT's accuracy dropped to 90.3% and its recall to 89.7%. This is because DAGCN's dynamic topology module updates the association weight between the reactor and the cooling system in real time (from 0.8 under normal conditions to 0.95), quickly capturing failure propagation paths; while GAT uses a static topology with a fixed association weight of 0.8, which cannot adapt to changes in operating conditions. Under abnormal radiation conditions (a sudden increase in gamma-ray dose rate to 3 μSv/h), DAGCN achieved a recall rate of 96.1%, while random forest only achieved 76.3%-traditional models cannot identify the coupled risk of "abnormal radiation + decreased cooling flow rate," while DAGCN, through a multi-source attention module, increases the weight of the radiation index from 0.78 to 0.9, prioritizing the identification of this extreme signal (Figure 2).

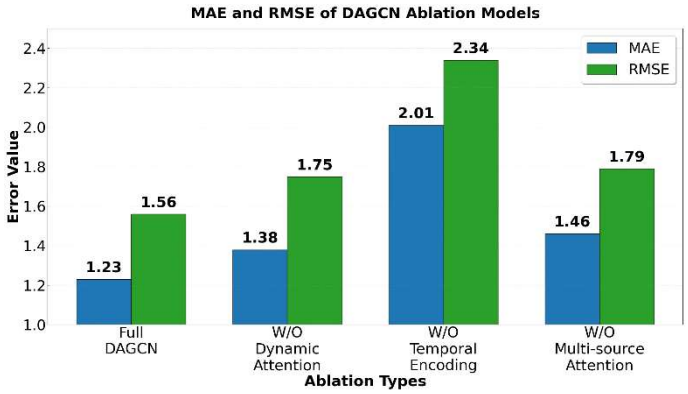


Figure 2. Comparison of MAE and RMSE for Ablation Models.

Figure 3 shows a line graph comparing the accuracy of each model under normal and extreme operating conditions. The horizontal axis represents the operating condition type (normal, sudden temperature rise, pressure fluctuation, radiation anomaly), and the vertical axis represents the accuracy (80%-100%). Different colored lines represent different models. As

can be seen from the graph, the red line of DAGCN consistently maintains the highest accuracy, with the smallest fluctuations between operating conditions (95.8%-98.2%). The purple line of Random Forest exhibits the largest fluctuations, dropping to 82.1% under the radiation anomaly condition. The blue line of GAT consistently falls below 92% under extreme operating conditions, significantly lower than DAGCN. This result demonstrates that DAGCN's dynamic topology update and attention mechanism can effectively adapt to extreme operating conditions, meeting the assessment needs of nuclear fuel cycle facilities for complex scenarios.

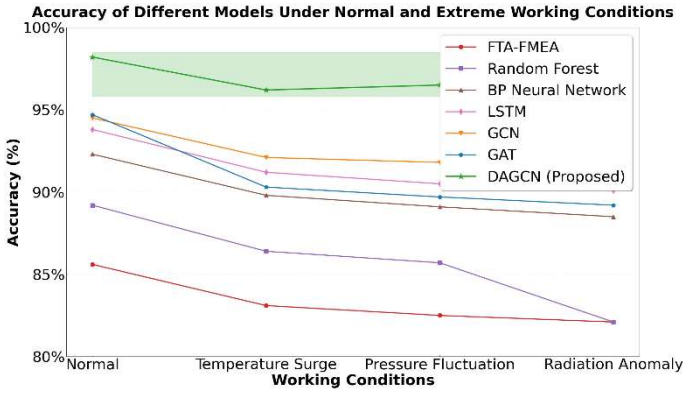


Figure 3. Accuracy Comparison of Various Models under Normal and Extreme Operating Conditions.

4. Conclusion

This paper addresses the traditional technical pain points in reliability assessment of nuclear fuel cycle facilities by proposing the DAGCN model and completing experimental verification. The core research results are as follows: First, the overall performance of the model is significantly better than traditional methods and other deep learning models, achieving a test set accuracy of 98.2% and a recall of 97.8%, meeting the stringent requirements of nuclear facilities for high-risk identification. It can reduce 10 false positives and 4 high-risk false negatives, significantly reducing operational risks based on an average of 288 monitoring data points per day. The regression indicators MAE 1.23 and RMSE 1.56 are over 54% lower than traditional random forests, achieving accurate quantification of reliability scores. Second, ablation experiments verify the necessity of each module: the absence of the dynamic attention module leads to a 5.3 percentage point decrease in recall, while the absence of the temporal coding module leads to a 63.4% increase in MAE; these two are the core of the model. The multi-source attention module mainly optimizes feature quality and has a relatively small impact on performance. Third, it exhibits outstanding adaptability to extreme operating conditions. DAGCN maintains an accuracy rate exceeding 95.8% even under scenarios involving sudden temperature increases and abnormal radiation. Its dynamic topology update and attention mechanism can quickly capture failure propagation paths, overcoming the limitations of traditional static evaluation models. In summary, DAGCN effectively overcomes the technical bottlenecks of multi-source data fusion, dynamic correlation capture, and temporal failure learning, providing crucial support for the digital and intelligent development of reliability assessment for nuclear fuel cycle facilities.

References

[1] Peng, M., Feng, W., Cao, Q., Hu, Y., Chen, Y., & Wang, D. (2022). Research progress on the application of Raman spectroscopy in nuclear fuel analysis. The Journal of Light Scattering, 34, 85–94.

[2] Jiao, Y., Yu, J., Zhou, Y., Li, Y., Chen, P., & Duan, Z. (2022). Research and development progress and application prospects of commercial pressurized water reactor nuclear fuel. Nuclear Power Engineering, 43, 1–7.

[3] Dong, Y., Lü, J., & Li, Q. (2024). Analysis of the influence of particle agglomeration behavior on the failure of dispersed nuclear fuel cores. Atomic Energy Science and Technology, 58, 868–877.

[4] Fang, Q., Lu, Y., Hou, C., & Dai, Z. (2025). Seismic design requirements for equipment in my country's civil nuclear fuel cycle facilities and their comparison with relevant international standards. Earthquake Disaster Prevention Technology, 20, 362–371.

[5] Zhang, Y., Zhao, X., Zhang, Y., Yang, Y., Lü, W., Liu, X., ... & Ge, C. (2025). Research progress on the antioxidant mechanism and performance enhancement of accident-resistant nuclear fuel UN. Journal of Engineering Science, 47, 682–696.

[6] Wang, H., & Hanzhou, R. (2025). Study on bolt seizure of nuclear fuel transport container under bias load. Engineering Research and Application, 3, 7–9.

[7] Sheng, H., He, J., Gou, J., Shan, J., & Liu, G. (2024). Improvement of radiolysis gas model for critical accident analysis of nuclear fuel solution system. Nuclear Power Engineering, 45, 160–165.

[8] An, J., Chen, B., Xie, Z., Zhang, X., Bi, Y., & Lu, L. (2024). Research on key technologies for the development of resistance welding equipment for nuclear fuel rods. Electric Welding Machine, 54, 44–49.

[9] Liu, X., He, L., Wu, M., Wei, G., Li, Z., Li, Y., ... & Chen, D. (2021). Research on experimental method of indirect neutron CT for nuclear fuel elements based on neutron IP plate. Atomic Energy Science and Technology, 55, 939–944.

[10] Wang, F., Xie, D., Zhang, A., Kang, R., Wu, L., & Pan, H. (2021). Comparative study on static and dynamic force analysis during nuclear fuel fission and fragmentation. Journal of Chongqing University of Technology (Natural Science), 35, 100–105.

[11] Liu, T. (2021). Research on particle size characterization method of graphite powder for nuclear fuel elements of high-temperature gas-cooled reactor. Nuclear Science and Engineering, 41, 689–694.